

Electrochemical and Antioxidant Properties of Biogenic Silver Nanoparticles

Arif Ullah Khan¹, Yun Wei¹, Zia Ul Haq Khan¹, Kamran Tahir¹, Shahab Ullah Khan², Aftab Ahmad¹, Faheem Ullah Khan¹, Li Cheng¹, Qipeng Yuan^{1*}

¹*State Key Laboratory of Chemical Resource Engineering, Beijing University of Chemical Technology, Beijing, PR China

²Department of Physics, University of Peshawar, 25000, Pakistan

*E-mail: yuanqp@mail.buct.edu.cn

Received: 15 June 2015 / Accepted: 27 July 2015 / Published: 26 August 2015

The Present Bio-synthesis is an efficient, fast, cheap, nontoxic, simple and eco-friendly protocol for silver nanoparticles synthesis, which is more beneficial than commonly used physiochemical methods. Here in silver nanoparticles are biosynthesized using *Citrus sinensis var. Kozan yerly* fruit juice as reducing and stabilizing agent. The X-ray diffraction (XRD) pattern confirms the crystalline nature of silver nanoparticles. The high resolution transmission electron microscopy confirmed that the silver nanoparticles are of average 4-10 nm particle size. The UV-vis absorption spectrum shows a characteristic surface plasmon resonance absorption peak of silver nanoparticles at 443 nm. FTIR confirmed phytochemicals of *Citrus sinensis var kazan yerly* fruit juice involved in the synthesis and stabilization of silver nanoparticles. Furthermore, the silver nanoparticles modified electrode (Ag/GC) exhibited an excellent electro-catalytic activity toward the red-ox reaction of phenolic compounds (Catechol) and DPPH free radical scavenging activity. The synthesized silver nanoparticles are stable and comparable in size. These silver nanoparticles showed potential applications in the fields of electrochemistry, sensors, catalysis, nanodevices and medical.

Keywords: Electro-catalytic, Bio-syntheses, Silver nanoparticles, *Citrus sinensis var. Kozan yerly*, Antioxidant

1. INTRODUCTION

The synthesis of noble-metal (Au, Ag and Cu) nanoparticles with controllable particle size and shape, is of great interest because such nanoparticles patterns provide the possibility of developing different functional devices with optical, sensing, and electrical properties [1]. Nanoparticles have great importance than their bulk materials because of their unique mechanical, physical, optical and

electromagnetic properties which are based upon size, dispersion and morphology of Nanoparticles. Nanoparticles exhibit a high surface to volume ratio with decreasing size, which plays an important role in catalytic activity and other related properties such as antimicrobial activities of Ag nanoparticles. Chemical method is the most important among the different methods employed for the syntheses of nano particles [2]. However, the use of lethal chemicals cannot be avoided by these methods of synthesis of nanoparticles. Platinum, Gold and silver nano particles are broadly used in daily life such as soaps, shampoos, detergents, cosmetic products, shoes, and toothpastes as well as medical and pharmaceutical fields [3]. Therefore, it is the need of time to develop green or eco-benign protocols for nanoparticles synthesis that do not require toxic chemicals and depend upon the naturally occurring nonlethal compounds. Nanoparticles can be synthesized by biological methods using microorganisms [4, 5], enzymes [6] and plant extracts (natural compounds) which are considered as possible green or eco-benign alternatives to chemical and physical methods. The use of plant extracts for nanoparticles synthesis is favorable and beneficial over other biological methods such as microbial protocol, because it does not require the complex process of maintaining cell cultures and can also be suitable to scale up for large scale synthesis [7].

Citrus fruits and derived products from them have been well known to have beneficial effects on human health owing to their high concentration of vitamin C and bioactive compounds such as phenolic acid, flavonoid, limonoid, carotenoid and fiber [8, 9]

Plants have a number of reducing agents such as poly phenols and flavonoids etc. which takes place the reduction of Ag^+ ions. These poly phenols and flavonoids are used as antimicrobial and antioxidant agents by the plants to protect themselves from various pathological conditions. *Citrus sinensis var. kozan yerly* fruit juice has been investigated for phytochemical investigation and it was reported that plant is rich in several poly phenols and other bioactive compounds [10]. In this study we synthesized Ag nanoparticles using fruit extract of *Citrus sinensis var. kozan yerly* on time scale (≤ 100 min), which is faster or equivalent to some of the currently used chemical methods. The less time processing, well dispersion, spherical, small sized (4-10nm) nano particles synthesis, efficient electrocatalytic and antioxidant properties ensures the study prominent than other biological methods for silver nanoparticles synthesis.

2. MATERIALS AND METHODS

2.1. Preparation of Orange extract

Citrus sinensis var. kozan yerly was purchased from market and peeled out. The juice was quenched using juice extractor and filtered with whatman No:1 filter paper. The filtrate was centrifuged again at 10000 rpm for 10 minutes at 4°C to remove the remaining solid materials. The supernatant was used for the synthesis and stabilization of silver nanoparticles.

2.2. Synthesis of Ag nanoparticles

For the synthesis of Ag nanoparticles, 20 ml of *Citrus sinensis* var. *kozan yerly* fruit extract was added to 50 ml of 6×10^{-3} M aqueous solution of AgNO_3 (sigma Aldrich) in 100ml beaker. The beaker was placed on magnetic stirrer and stirred at 25 °C to ensure the complete mixing.

The Ag nanoparticles suspension thus obtained was centrifuged at 10,000 rpm for 15 min followed by re-dispersion of the pellet in de-ionized water. Then the supernatant was discarded and the pallet (Ag nanoparticles) was freeze dried using VirTis freeze mobile 6ES freeze drier.

2.3. Characterization studies

UV-2450 spectrophotometer (Shimadzu) at a resolution of 1nm in the wavelength range of 350-800 nm was used to monitor the Biosynthesis of silver nanoparticles. The X-ray diffraction (XRD) pattern was studied by Rigaku Miniflex X-ray diffracto meter at $10-70^\circ$. A Hitachi EDX elemental microanalysis system and JEOL3010 high resolution transmission electron microscope were used to study the morphology, size and crystalline nature of the Ag nanoparticles. Infra red (IR) spectrum of Ag nanoparticle was obtained using the KBr pellet technique on an ABB MB3000 spectrophotometer where it was scanned between 2000 and 500 cm^{-1} at a resolution of 4 cm^{-1} in transmittance mode.

2.4. Assembling of AgNPs modified glassy carbon electrode

The bare glassy carbon electrode (GCE) was polished into a mirror-like surface with 0.5 and 0.05 mm alpha Al_2O_3 and then rinsed ultrasonically with water bath, so that any physically adsorbed species is removed. The cleaned GC electrode was modified by dip coating with silver nanoparticles, using immersion times (2 h) in the colloidal nanoparticles solutions.

2.5. Electrocatlytic activity of AgNPs modified glassy carbon electrode

The modified electrode was electrochemically characterized by cyclic voltammetry (CV) in 0.15M sodium acetate solution as electrolyte aqueous medium. Electrocatalytic activity of biogenic AgNPs was determined by cyclic voltammetry (CV). The CV responses of phenolic compound catechol $\text{C}_6\text{H}_6\text{O}_2$ in 0.15M sodium acetate solution at the glassy carbon electrode (GCE) vs saturated calomel electrode (SCE) at room temperature and AgNPs assembled GC electrode vs SCE was monitored.

2.5. Antioxidant assay

Antioxidant assay for Ag nanoparticles was performed as previously reported [11] with a slight modification. Different concentrations (0.031, 0.062, 0.125, 0.250, 0.5 and 1mg/ml) of Ag nanoparticles were individually mixed with 0.5ml of 1mM DPPH and incubated in dark for 30

minutes. After incubation the absorbance of the samples was determined by UV 1100 spectrophotometer (MAPADA instruments) at 517nm against methanol as a blank. DPPH methanol reagent without sample was used as control and Vit.C was used as standard. The percentage of inhibition was calculated according to the following formula.

$$\% \text{ of inhibition} = \frac{[\text{Absorbance}_{\text{control}} - \text{Absorbance}_{\text{test}}] / \text{Absorbance}_{\text{control}} \times 100}$$

3. RESULTS AND DISCUSSION

The present work was aimed to investigate the biosynthesis, subsequent characterization, electrocatalytic and antioxidant properties of silver nanoparticles. The biosynthesis of silver nanoparticles was observed based on visual observation of the color change from yellow to dark black within 30 min, followed by monitoring the rate of biosynthesis using UV spectrophotometer (Shimadzu 2450). The fruit extract of *Citrus sinensis var. kozan yerly* in the absence of AgNO_3 was used as control and no color change was observed in control.

This color appears due to SPR in Ag nanoparticles. The characteristic SPR peak was not observed at the initial stage but after 20 minutes the free electrons of silver nanoparticles give rise to SPR peak [12].

3.1 UV-Vis spectroscopy

The rate of Ag nanoparticles biosynthesis was monitored using UV- visible spectroscopy. The monitoring of UV- vis spectra was time dependant (**Fig.1**). **Fig.1** clearly shows that with increase in contact time the intensity and sharpness of SPR peak increases. SPR showed the maximum absorbance at 447 nm. SPR peak depends upon the size, shape dispersion and the surrounding media of silver nanoparticles. SPR gives rise to peak which is well-documented for various metallic nano particles ranging from 2 nm to 100 nm [13].

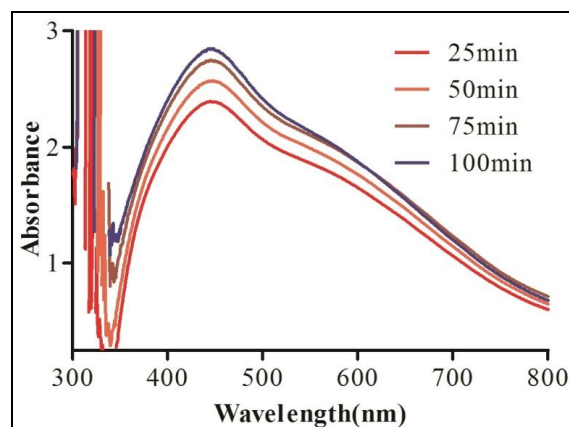


Figure 1. Time dependent UV-Vis Spectra of Ag nanoparticles

3.2 XRD pattern

X-ray diffraction analysis at 10° - 70° (**Fig.2**) confirmed the crystalline nature of Ag nanoparticles. Different numbers of Bragg reflection with 2θ values of 38.03° , 46.18° , 63.43° represent to the (111), (200) and (220) set of lattice planes (**Fig.2**). Which are in agreement with JCPDS file number 00-004-0783 and may be indexed to the face centered cubic (fcc) structure of Ag nanoparticles. The peak corresponding to (111) is more intense than the other planes suggesting that (111) is the predominant orientation as confirmed by the HRTEM measurements. The peaks which are unassigned may be due to the crystallization of bioorganic materials that capped on the surface of Ag nano particles.

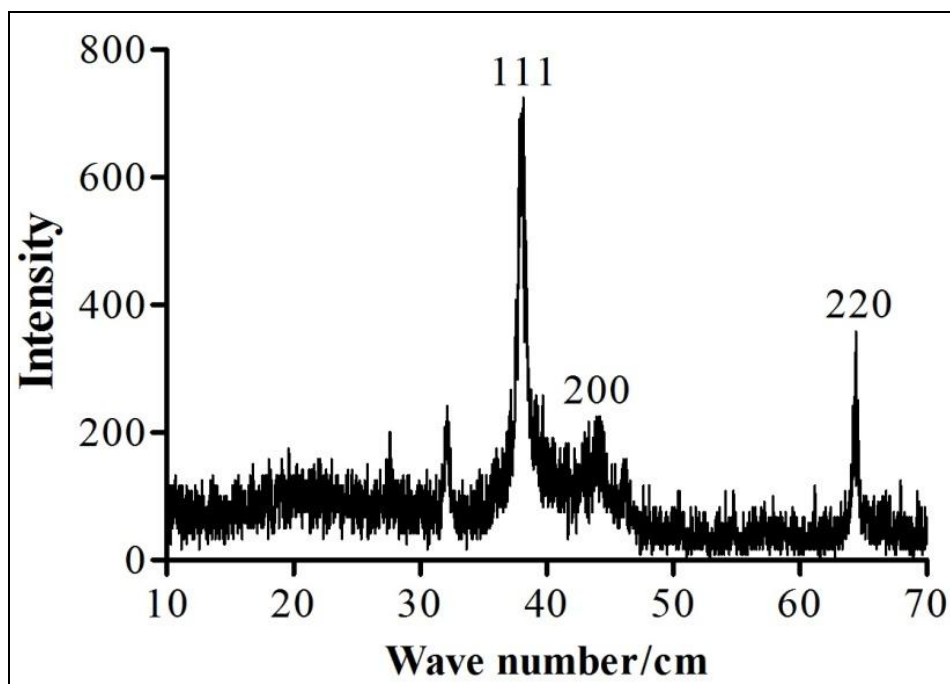


Figure 2. XRD pattern of Ag nanoparticles

3.3 EDX profile

The EDX profile confirmed the elemental composition of Ag nanoparticles and indicated strong signals for Silver atoms in the range of 3keV which is typical signal of the absorption of metallic and spherical Silver nanocrystals due to surface plasmon resonance [14, 15] as shown in **fig.3**. There is no ionic silver (Ag^+) peak which confirms that all the Ag^+ are reduced to Ag^0 resulting in good yield of silver nanoparticles. The EDX pattern clearly shows that the Ag nano particles are crystalline in nature, which is caused by the reduction of silver ions using *Citrus sinensis var kozan yerly* fruit extract.

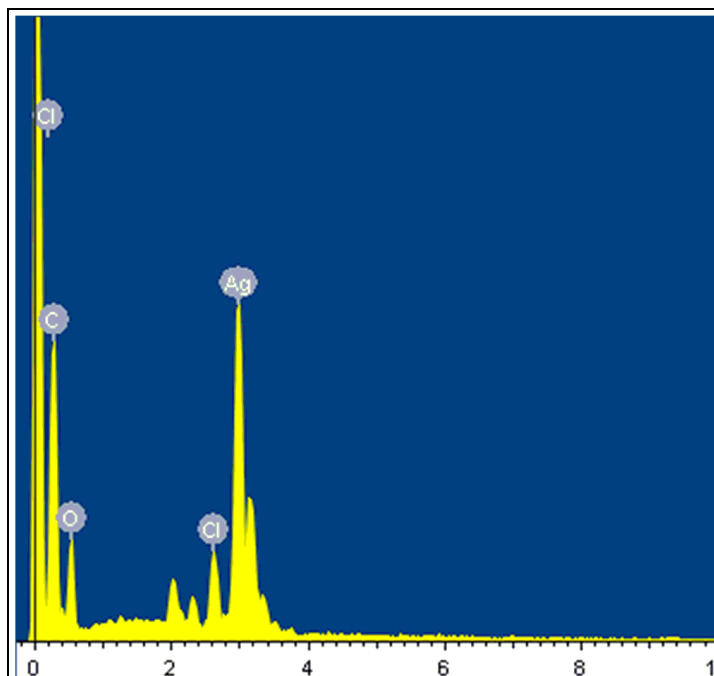


Figure 3. EDX profile of Ag nanoparticles

3.4 High resolution transmission electron microscopy (HRTEM)

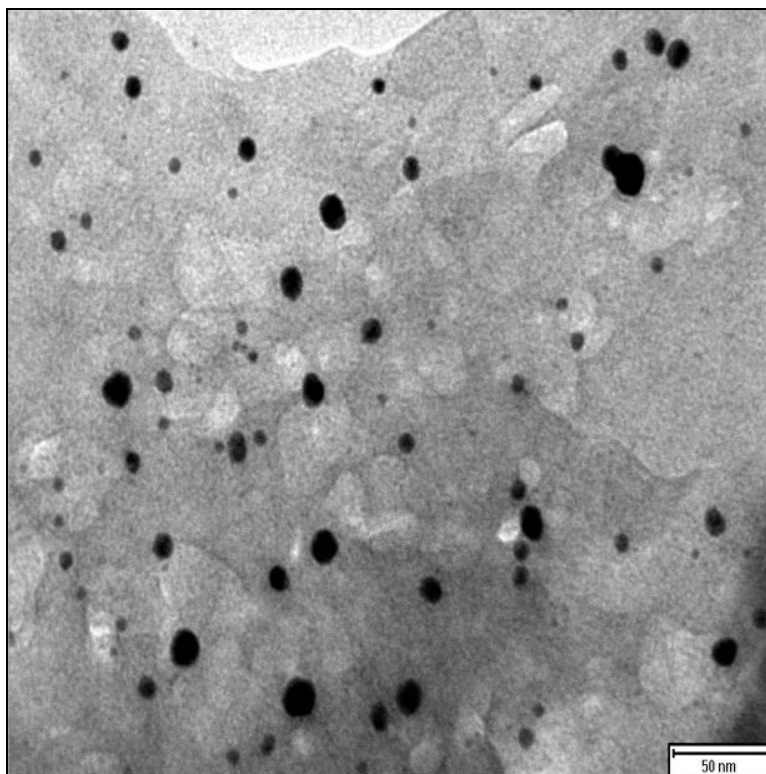


Figure 4. HRTEM image of Ag nanoparticles

HRTEM was performed to determine the dispersion, size, shape and morphology of synthesized silver nanoparticles. It is clear from the HRTEM image that the morphology of the silver nanoparticles is spherical which is in agreement with the shape of SPR band in UV-vis spectra. The average particle size measured from the HRTEM images is to be 4-10 nm which is in good agreement with the particle size calculated from XRD analysis. It is also cleared from the HRTEM image that the silver nano particles are spherical and highly dispersed and there is no aggregation among them (**Fig.4**). Which are in close agreement with EDX findings. The smaller, spherical particle size and well dispersion of silver nano particles leads to more active sites and large surface area which are responsible for its efficient antibacterial, electrocatalytic and antioxidant properties [16, 17]. The white lining around the Ag nanoparticles show the appearance of capping and stabilizing agents (organic compounds).

3.5 FTIR analysis

FTIR analysis (**Fig.5**) indicated the possible naturally occurring organic molecules, taken part in stabilization and capping of the Ag nanoparticles FTIR spectrum shows absorption bands at 3370, 2860, 1580, 1190 and 1010 cm^{-1} (**Fig.5**). The absorption bands at 3370 cm^{-1} and 2860 cm^{-1} represent the OH group stretching and sp² C-H (alkane) vibration respectively. The absorption at 1580 cm^{-1} was attributed to the C=C symmetric stretching vibration of aromatic rings. The absorption band at 1190 cm^{-1} was attributed to the C-N stretching vibration. The absorption band at 1010 cm^{-1} might is contributed by the C-O group of the polysaccharides in the fruit juice of *Citrus sinensis var. kozan yerly*. It is assumed that -OH group present (indicated in FTIR) in the *Citrus sinensis var. kozan yerly* is responsible for the reduction of silver ions to elemental silver nanoparticles through the oxidation of alcohol to aldehydic group. For example

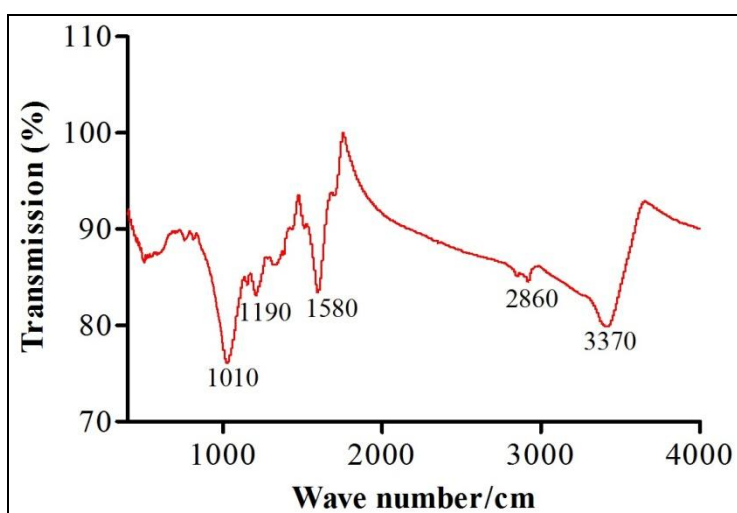
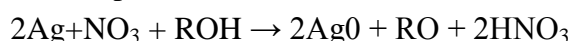


Figure 5. FTIR spectra of Ag nanoparticles

3.6. Electrochemical behavior of catechol at Ag-NPs modified electrode

Electrocatalytic activity of biosynthesized AgNPs was determined by cyclic voltammetry (CV). **Figure 6 (A)** show CV responses of phenolic compound catechol $C_6H_6O_2$ at glassy carbon electrode (GCE) vs saturated calomel electrode (SCE) and figure 6 (B) show CV of AgNPs assembled GC electrode vs SCE. The **fig. A** showed one anodic peak and one cathodic peak of equal intensity. The redox couple of I_{pA}/I_{pC} is equal to unity [18-21], which means that during electrolytic process, the catechol (**1a**) is oxidized to highly reactive species quinone (**2a**) and the red-ox couple shows the stability of the quinone on the surface of electrode. In figure **B** there are two another anodic peaks (A_1 and A_2) appeared at higher potential as compare to first one because of photolytic free radical reaction as shown in scheme 1. From the figure **B** it is clear that red-ox couple of I_{pA}/I_{pC} is not equal to unity, very little **1a** was converted to **2a**, which cause polymerization or hydroxylation.

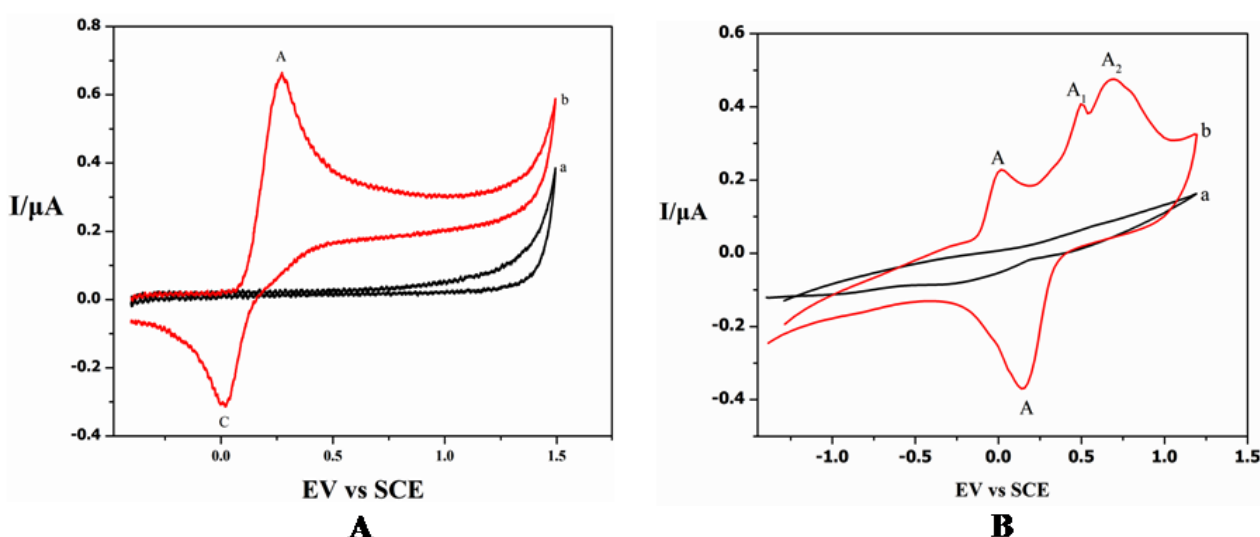


Figure 6. (A) Cyclic voltammograms of catechol on GC electrode in 0.15M sodium acetate solution. at scanning rate 50 mV-s⁻¹ vs SCE at 25°C. (a) blank acetate solution (b) catechol, (B) Cyclic voltammograms of catechol on AgNPs –assemble GC electrode in 0.15M sodium acetate solution (a) blanks acetate solution (b) catechol at scanning rate 50 mV-s⁻¹ vs SCE at 25°C.

Figure 7C showed the effect of scanning on red-ox couple of catechol. From figure C we observed that increase in scan rate, the anodic and cathodic peaks are decreased, it showed the stability of ortho quinone on the surface of Ag assembled GC electrode. From the figure 7C, there is one extra cathodic peak (C1) appear at potential 0.3V, which is due to non-conducting layer formed on the surface of electrode [22]. Two cathodic peaks (C and C1) were observed in figure 7C. At low scan rates, the peak current ratio, I_{pA}/I_{pC} is greater than unity, while it decreases gradually with increasing V and approaches unity [23]. Moreover, at high scan rates, only peak C remains and cathodic peak C1 disappears. On the other hand, even at very low scan rates, the peak separation (E_{pA}/E_{pC}) exceeds the expected 2e⁻ reversible process. Hence, assuming the proton transfer involved in the redox reaction of quinones is a fast process, we suggest that peaks A and C are indicative of a quasi-reversible charge

transfer process corresponding to the catechol (1a) o- benzoquinone (2a) system. Further we proceeded to study potential stability of biosynthesized AgNPs assembled GC electrode vs SCE at 50 mV-s⁻¹ as shown in figure 7D.

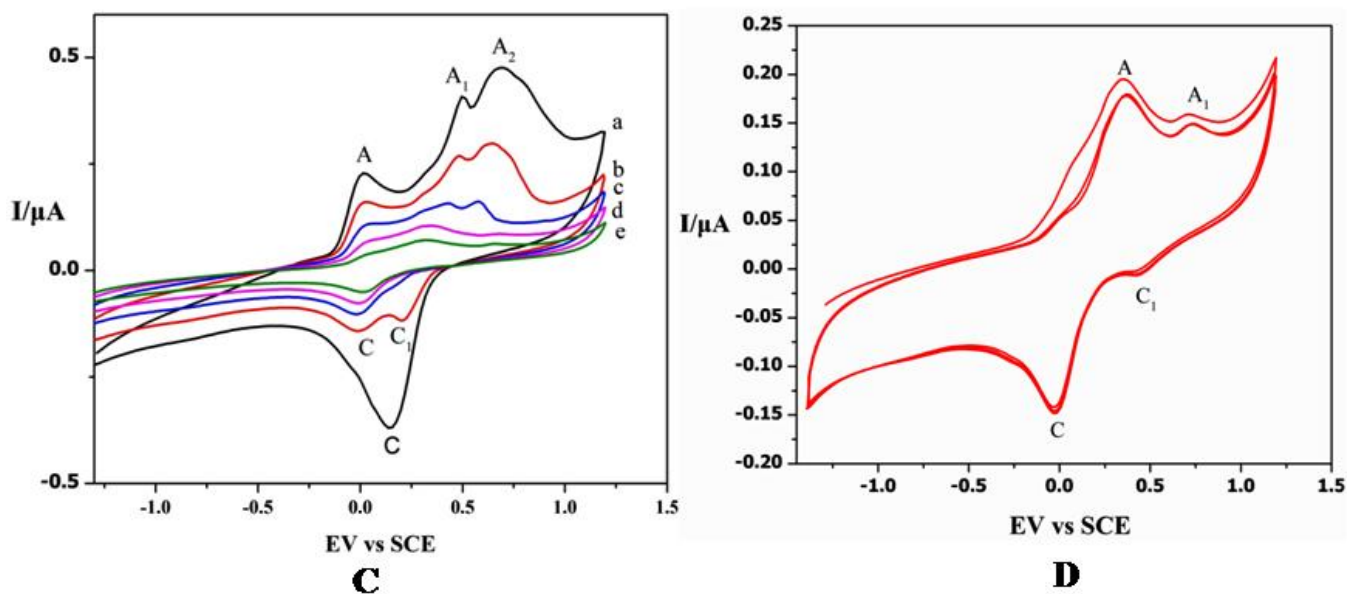
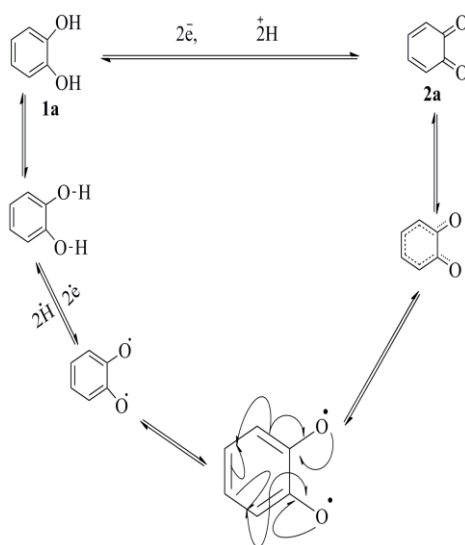


Figure 7. (C) Cyclic voltammograms of catechol on AgNPs -assemble GC electrode in 0.15M sodium acetate solution at different scanning rates (a) 100 (b) 80 (c) 60 (d) 40 (e) 20 mV-s⁻¹ vs SCE at 25°C, (D) Multi Cyclic voltammograms of catechol on AgNPs–assemble GC electrode in sodium acetate solution at scanning rate 50 mV-s⁻¹ vs SCE at 25°C.



Scheme 1. Electrochemical Anodic Red-Ox reaction of Catechol using AgNPs assembled GC electrode in the presences of 0.15 M sodium acetate as electrolyte at room temperature.

In multi cyclic voltammetry we observed that during the 1st, 2nd and 3rd scan there is no change in the intensity and position of red-ox peaks. In each cycle the anodic and cathodic peaks are same, which shows the stability of Ag assembled GC electrode. On the basis of all these observation we proposed the following mechanism for the electrochemical red-ox reaction of phenolic compounds (Catechol) in to reactive species o-quinone as shown in scheme 1.

3.7. Antioxidant activity of Ag nanoparticles

Antioxidant activity of Ag nanoparticles was assessed by DPPH free radical scavenging assay, using Vit.C as positive control. DPPH is a stable compound and accepts hydrogen or electrons from silver nanoparticles. The results obtained in the antioxidant assay showed effective free radical scavenging by Ag nanoparticles (**Fig.8**). Six different concentrations were monitored in this study and we noted that the activity increased with increasing concentrations of AgNPs. Similar observations with enhanced DPPH scavenging activity by selenium, platinum, silver nanoparticles [24, 25] and by torolex and chitosan coated gold nano particles have been reported [25, 26]. The antioxidant property has been proved by some researchers to be related with the development of reducing power. Reductones, which have strong reducing power, are generally believed not only to react directly with peroxides but also to prevent peroxide formation by reacting with certain precursors [27]. Silver nanoparticles are suggested to act as electron donors, reacting with free radicals to convert them to more stable products, which can terminate radical chain reaction. Moreover, the reducing power of Ag nanoparticles correlated well with the radical scavenging activity.

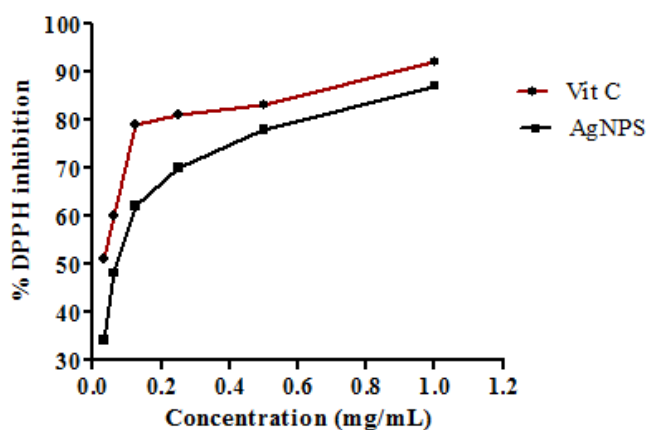


Figure 7. Antioxidant activity of Ag nanoparticles

4. CONCLUSION

In this work, highly dispersed, stable and electrochemically active silver nanoparticles (average size 4-10 nm) were synthesized using *Citrus sinensis var kozan yerly* fruit juice by bio-green method, a

cost effective and eco-friendly protocol. The new application of silver nanoparticles onto the GC electrode is proposed. The uniform and high surface areas onto the GC electrode facilitate its' use for electro-catalytic applications. The resulting silver nanoparticles assembled GC electrode show an excellent electro-catalytic response towards the red-ox reaction of phenolic compounds. Silver nanoparticles showed very good electro-catalytic performance with low cost and sensitivity. Thus the AG/GC has attractive electro-catalytic properties for the red-ox reaction of phenolic compounds and other red-ox reactions or applications. Furthermore silver nanoparticles are found to have significant DPPH free radical scavenging properties. This could be result as an eco-friendly for electronic applications, cancer treatment, sensors, drug delivery and other medical applications. The outcomes of this study illustrate a broad range of applications of electrochemically and bioactive silver nanoparticles.

ACKNOWLEDGMENTS

The authors are thankful to China Scholarship Council (CSCNo: 2013GXZ036) for support of this research work.

References

1. Renáta Orináková, Lenka Škantárová, Andrej Orinák, Jakub Demko, Miriam Kupková, Jan T. Andersson, *Int. J. Electrochem. Sci.*, 8 (2013) 80 - 99
2. S. Sundarajan, A.R. Chandrasekaran, S. Ramakrishna, *J Am Ceram Soc.*, 93 (2010) 3955-3975.
3. D.R. Bhumkar, H.M. Joshi, M. Sastry, V.B. Pokharkar, *Pharm res.*, 24 (2007) 1415-1426.
4. V.C. Verma, R.N. Kharwar, A.C. Gange, *Nanomedicine.*, 5 (2010) 33-40.
5. Y. Konishi, K. Ohno, N. Saitoh, T. Nomura, S. Nagamine, H. Hishida, Y. Takahashi, T. Uruga, *J Biotech*, 128 (2007) 648-653.
6. I. Willner, R. Baron, B. Willner, *Adv Mater.*, 18 (2006) 1109-1120.
7. S.S. Shankar, A. Rai, A. Ahmad, M. Sastry, *J. Colloid Interface Sci.*, 275 (2004) 496-502.
8. S. Gorinstein, O. Martín-Belloso, Y.-S. Park, R. Haruenkit, A. Lojek, M. Číž, A. Caspi, I. Libman, S. Trakhtenberg, *Food Chem.*, 74 (2001) 309-315.
9. M.A. Anagnostopoulou, P. Kefalas, E. Kokkalou, A.N. Assimopoulou, V.P. Papageorgiou, *Biomed. Chromatogr.*, 19 (2005) 138-148.
10. E. Agcam, A. Akyıldız, G.A. Evrendilek, *Food Chem.*, 143 (2014) 354-361.
11. C.W. Choi, S.C. Kim, S.S. Hwang, B.K. Choi, H.J. Ahn, M.Y. Lee, S.H. Park, S.K. Kim, *Plant Sci.*, 163 (2002) 1161-1168.
12. M. Noginov, G. Zhu, M. Bahoura, J. Adegoke, C. Small, B. Ritzo, V. Drachev, V. Shalaev, *Appl. Phys. B.*, 86 (2007) 455-460.
13. M. Gutierrez, A. Henglein, *J Phy Chem.*, 97 (1993) 11368-11370.
14. P. Magudapathy, P. Gangopadhyay, B. Panigrahi, K. Nair, S. Dhara, *Phy B: Cond Mat.*, 299 (2001) 142-146.
15. S. Muthukrishnan, S. Bhakya, T.S. Kumar, M. Rao, *Ind Crop and Prod.*, 63 (2015) 119-124.
16. K. Mogyorósi, N. Balázs, D. Srankó, E. Tombác, I. Dékány, A. Oszkó, P. Sipos, A. Dombi, *Appl Cat B: Env.*, 96 (2010) 577-585.
17. S. Saha, A. Pal, S. Kundu, S. Basu, T. Pal, *Langmuir*, 26 (2009) 2885-2893.
18. Nematollahi, D.; Golabi, S. M. *J. Electroanal. Chem.*, 405 (1996) 133-140.
19. Zia Ul Haq Khan, Yongmei Chen, Shafiullah Khan Dandan Kong Mo Heng Liang Pingyu Wan,

Int. J. Electrochem. Sci., 9 (2014) 4665 - 4674

20. Nematollahi, D.; Golabi, S. M. *J. Electroanal. Chem.*, 481 (2000) 208-214.
21. Zia Ul Haq Khan, Arif Ullah Khan, Yongmei Chen, Shafiullah Khan, Dandan Kong , Karman Tahir, Faheem Ullah Khan, Pingyu Wan and Jin Xin. *Tetrahedron.*, 71 (2105) 1674-1678
22. Silverstein R, Webster M FM. *Spectrometric.*, Wiley: NewYork. 6th ed (1998). 217-249
23. D. Nematollahi, S.M. Golabib. *J. Electroanal. Chem.*, 481 (2000) 208–214
24. X. Gao, J. Zhang, L. Zhang, *Adv Mater.*, 14 (2002) 290.
25. Z. Nie, K.J. Liu, C.-J. Zhong, L.-F. Wang, Y. Yang, Q. Tian, Y. Liu, *Free Radical Biol. Med.*, 43 (2007) 1243-1254.
26. D. Raghunandan, M.D. Bedre, S. Basavaraja, B. Sawle, S. Manjunath, A. Venkataraman, *Colloids Surf., B*, 79 (2010) 235-240.
27. D.-Z. Xia, X.-F. Yu, Z.-Y. Zhu, Z.-D. Zou, *Nat Prod Res.*, 25 (2011) 1893-1901.

© 2015 The Authors. Published by ESG (www.electrochemsci.org). This article is an open access article distributed under the terms and conditions of the Creative Commons Attribution license (<http://creativecommons.org/licenses/by/4.0/>).